EBioMedicine 13 (2016) 201–211

Contents lists available at ScienceDirect

EBioMedicine

journal homepage: www.ebiomedicine.com

Research Paper

Fenofibrate Inhibits Cytochrome P450 Epoxygenase 2C Activity to Suppress Pathological Ocular Angiogenesis

Yan Gong [a], Zhuo Shao [a], Zhongjie Fu [a], Matthew L. Edin [b], Ye Sun [a], Raffael G. Liegl [a], Zhongxiao Wang [a], Chi-Hsiu Liu [a], Samuel B. Burnim [a], Steven S. Meng [a], Fred B. Lih [b], John Paul SanGiovanni [c], Darryl C. Zeldin [b], Ann Hellström [d], Lois E.H. Smith [a,*]

[a] Department of Ophthalmology, Boston Children's Hospital, Harvard Medical School, Boston, MA 01248, United States
[b] Division of Intramural Research, National Institute of Environmental Health Sciences, National Institutes of Health, Research Triangle Park, NC 27709, United States
[c] Section on Nutritional Neurosciences, Laboratory of Membrane Biophysics and Biochemistry, National Institute on Alcohol Abuse and Alcoholism, National Institutes of Health, Bethesda, MD 20892, United States
[d] Department of Ophthalmology, Sahlgrenska Academy at University of Gothenburg, Gothenburg 40530, Sweden

ARTICLE INFO

Article history:
Received 3 August 2016
Received in revised form 23 September 2016
Accepted 28 September 2016
Available online 30 September 2016

Keywords:
Fenofibrate
Choroidal neovascularization
Retinopathy
Retinal neovascularization
Cytochrome P450 epoxygenase 2C
Omega-3 long-chain polyunsaturated fatty acids

ABSTRACT

Neovascular eye diseases including retinopathy of prematurity, diabetic retinopathy and age-related-macular-degeneration are major causes of blindness. Fenofibrate treatment in type 2 diabetes patients reduces progression of diabetic retinopathy independent of its peroxisome proliferator-activated receptor (PPAR)α agonist lipid lowering effect. The mechanism is unknown. Fenofibrate binds to and inhibits cytochrome P450 epoxygenase (CYP)2C with higher affinity than to PPARα. CYP2C metabolizes ω-3 long-chain polyunsaturated fatty acids (LCPUFAs). While ω-3 LCPUFA products from other metabolizing pathways decrease retinal and choroidal neovascularization, CYP2C products of both ω-3 and ω-6 LCPUFAs promote angiogenesis. We hypothesized that fenofibrate inhibits retinopathy by reducing CYP2C ω-3 LCPUFA (and ω-6 LCPUFA) pro-angiogenic metabolites. Fenofibrate reduced retinal and choroidal neovascularization in *PPARα*-/-mice and augmented ω-3 LCPUFA protection via CYP2C inhibition. Fenofibrate suppressed retinal and choroidal neovascularization in mice overexpressing human CYP2C8 in endothelial cells and reduced plasma levels of the pro-angiogenic ω-3 LCPUFA CYP2C8 product, 19,20-epoxydocosapentaenoic acid. 19,20-epoxydocosapentaenoic acid reversed fenofibrate-induced suppression of angiogenesis ex vivo and suppression of endothelial cell functions in vitro. In summary fenofibrate suppressed retinal and choroidal neovascularization via CYP2C inhibition as well as by acting as an agonist of PPARα. Fenofibrate augmented the overall protective effects of ω-3 LCPUFAs on neovascular eye diseases.

1. Introduction

Pathological ocular neovascularization causes vision loss in retinopathy of prematurity in children, in proliferative diabetic retinopathy in adults, and in age-related macular degeneration (AMD) in the elderly population (Hellstrom et al., 2013; Antonetti et al., 2012; Gibson, 2012). Neovascularization can be suppressed with anti-angiogenic agents, such as anti-vascular endothelial growth factor (VEGF) molecules (Cheung et al., 2012; Liu et al., 2015). However, anti-VEGF therapy can also suppress normal vessel growth and neuronal survival (Suzuki et al., 2011; Sato et al., 2012). Therefore, therapeutic agents inhibiting ocular neovascularization with fewer adverse effects are desirable.

Fenofibrate reduces serum cholesterol and triglyceride levels in patients at risk for cardiovascular disease such as those with diabetes mellitus (Keech et al., 2005). Fenofibrate also reduces the risk of proliferative diabetic retinopathy by 35–40% as noted in two intervention trials of >20,000 patients with type 2 diabetes mellitus, the Fenofibrate Intervention and Event Lowering in Diabetes (FIELD) and the Action to Control Cardiovascular Risk in Diabetes (ACCORD) studies (Keech et al., 2007; Group et al., 2010). The MacuFen study also suggests that fenofibrate treatment decreases volume of diabetic macular edema (Massin et al., 2014). The mechanism underlying the protective effect of fenofibrate on diabetic retinopathy is independent of its ability to initiate a peroxisome proliferator-activated receptor (PPAR) α-mediated lipid lowering effect (Bogdanov et al., 2015; Simo et al., 2015). There are no clinical

Abbreviations: AA, arachidonic acid; AMD, age-related macular degeneration; CNV, choroidal neovascularization; COX, cyclooxygenases; CYP, cytochrome P450 epoxygenase; DHA, docosahexaenoic acid; EDP, epoxydocosapentaenoic acid; EET, epoxyeicosatrienoic acid; EPA, eicosapentaenoic acid; HRMEC, human retinal microvascular endothelial cell; LCPUFA, long-chain polyunsaturated fatty acids; LOX, lipoxygenases; OIR, oxygen-induced retinopathy; PBS, phosphate buffered saline; PPAR, peroxisome proliferator-activated receptor; VEGF, vascular endothelial growth factor.

* Corresponding author at: 300 Longwood Avenue, Boston, MA 02115, United States.
E-mail address: lois.smith@childrens.harvard.edu (L.E.H. Smith).

http://dx.doi.org/10.1016/j.ebiom.2016.09.025

studies on the effects of fenofibrate on other neovascular eye diseases, although fenofibrate has been shown to have a potent anti-apoptotic effect in the ischemic retina, to suppress ischemia-induced endothelial progenitor cell mobilization and homing, and to inhibit angiogenesis in vivo and in vitro (Moran et al., 2014; Wang et al., 2014; Varet et al., 2003).

Fenofibrate is a well-known PPARα agonist, but an in vitro assessment of 209 frequently prescribed drugs and related xenobiotics suggests that it is also a potent inhibitor of cytochrome P450 epoxygenase (CYP)2C (Walsky et al., 2005). The affinity of fenofibrate to CYP2C is >10 times higher (EC50 = 2.39 ± 0.4 μM) than to PPARα (EC50 = 30 μM) (Schoonjans et al., 1996). We hypothesized that the suppressive effects of fenofibrate on retinopathy might be mediated through suppression of CYP2C pro-angiogenic metabolites. Important CYP2C substrates with respect to retinopathy are ω-3 and ω-6 long-chain polyunsaturated fatty acids (LCPUFAs). The major ω-3 and ω-6 LCPUFAs found in the eye are respectively docosahexaenoic acid (DHA, C22:6ω-3) and arachidonic acid (AA, C20:4ω-6) (Sangiovanni et al., 2009a). DHA is present in the retina at a higher concentration (20%) than in any other tissues (SanGiovanni and Chew, 2005; Sapieha et al., 2012).

LCPUFAs (and their biologically active pro and anti-angiogenic metabolites) influence the development of neovascular eye diseases (SanGiovanni and Chew, 2005; Sapieha et al., 2012; Stahl et al., 2011; Fu et al., 2016). Dietary intake of ω-3 versus ω-6 LCPUFAs is associated with suppression of pathological retinal angiogenesis in animal models for retinopathy of prematurity, proliferative diabetic retinopathy and AMD (Connor et al., 2007; Gong et al., 2015) with the implication that the sum total of ω-3 LCPUFA metabolites are anti-angiogenic. Bioactive ω-3 and ω-6 LCPUFA metabolites are produced by three major enzyme systems: the cyclooxygenases (COX), lipoxygenases (LOX) and CYPs. Although cyclooxygenase and lipoxygenase ω-6 LCPUFA-derived metabolites are generally pro-angiogenic, ω-3 LCPUFA-derived cyclooxygenase analogues are generally anti-angiogenic including prostaglandin E3, which inhibits endothelial tubule formation (Szymczak et al., 2008), and the 5-lipoxygenase metabolite 4-hydroxydocosahexaenoic acid mediates much of the anti-retinopathy effect of ω-3 LCPUFA diet in mouse retinopathy. 4-Hydroxydocosahexaenoic acid reduces retinal inflammation and inhibits endothelial cell functions by activating PPARγ (Sapieha et al., 2011). CYP2C metabolizes LCPUFAs to biologically active, pro-angiogenic epoxides (Tsao et al., 2001). While ω-3 LCPUFA products from the other metabolic pathways inhibit angiogenesis, CYP2C metabolites derived from ω-3 (and ω-6) LCPUFAs, such as 19,20-epoxydocosapentaenoic acid (EDP) and 14,15-epoxyeicosatrienoic acid (EET), promote retinal neovascularization(Shao et al., 2014), suggesting that CYP2C inhibition would be benefit neovascular eye diseases. We hypothesized that the inhibitory effect of fenofibrate on retinopathy (seen in the FIELD and ACCORD studies) is due to CYP2C inhibition and reduction in levels of pro-angiogenic CYP2C metabolites.

Current mouse models for diabetic retinopathy do not develop neovascularization. To evaluate fenofibrate effects on neovascular eye diseases we employed the mouse model of oxygen-induced retinopathy (OIR), which has reproducible and quantifiable retinal neovascularization similar to proliferative diabetic retinopathy as well as the laser-induced choroidal neovascularization (CNV) model of neovascular AMD(Smith et al., 1994; Gong et al., 2015). Fenofibrate suppressed both retinal and choroidal neovascularization in association with lowering the plasma levels of CYP2C metabolites and enhanced the protective effects of ω-3 LCPUFAs on pathological choroidal and retinal angiogenesis. This study suggested that fenofibrate suppressed neovascularization through both PPARα agonist activity and CYP2C inhibition.

2. Materials and Methods

2.1. Mice

Tie2-driven *CYP2C8* overexpressing transgenic mice were on a C57BL/6 background (Edin et al., 2011). Wild-type C57BL/6 mice were purchased from the Jackson Laboratory (000664, Bar Harbor, ME). For dietary experiments, the ω-6 LCPUFA AA and the ω-3 LCPUFAs DHA and eicosapentaenoic acid (EPA) were obtained from DSM Nutritional Products (TE Heerlen, Netherlands) and integrated into the rodent feed at Research Diets (New Brunswick, NJ) (Connor et al., 2007; Shao et al., 2014). The raw materials (TS00002988, DSM) were analyzed to confirm composition and the absence of peroxides, dioxin, benzopyrene or heavy metal contaminants (EPA1T1615.07/111001). The mice were fed a defined rodent diet with 10% (wt/wt) safflower oil containing either 2% ω-6 LCPUFA (AA) and no ω-3 LCPUFAs (DHA and EPA), or 2% ω-3 LCPUFAs and no ω-6 LCPUFA from postnatal day (P) 1 to P17 for the mouse model of OIR or from 7 days before laser photocoagulation for the laser-induced CNV model. All animal experiments complied with the Animal Research: Reporting of In Vivo Experiments (ARRIVE) guidelines, were carried out in accordance with the National Institutes of Health guide for the care and use of Laboratory animals (NIH Publications No. 8023, revised 1978), and were approved by the Boston Children's Hospital Animal Care and Use Committee.

2.2. Oxygen-induced Retinopathy

The mouse OIR model was used as described (Smith et al., 1994; Stahl et al., 2009; Connor et al., 2009; Stahl et al., 2010). Briefly to induce retinal neovascularization, mouse pups and their nursing mother were exposed to 75 ± 3% oxygen from P7 to P12. For the higher dose fenofibrate (F6020, Sigma-Aldrich, St. Louis, MO) treatment (100 mg/kg/day) fenofibrate was dissolved in corn oil (C8267, Sigma-Aldrich) to make 100 mg/ml solution and pure corn oil was used as vehicle control. For the lower dose treatment (10 mg/kg/day), fenofibrate was dissolved in 10% dimethyl sulfoxide (DMSO, D2650, Sigma-Aldrich) to make a 10 mg/ml solution and 10% DMSO was used as vehicle control. After return to room air, mice were orally gavaged with fenofibrate (100 or 10 mg/kg) or vehicle control daily from P12 to P16. At P17, eyes were enucleated immediately after euthanasia and fixed in 4% paraformaldehyde (P6148, Sigma-Aldrich) in phosphate buffered saline (PBS, 10010-023, Thermo Fisher Scientific, Waltham, MA) for 1 h at room temperature. Retinas were then dissected and stained overnight with Alexa Fluor 594 conjugated isolectin GS-IB_4 (10 μg/ml, I21413, Thermo Fisher Scientific) at room temperature. After washing with PBS, retinas were mounted onto microscope slides (12-550-15, Thermo Fisher Scientific) with photoreceptor side down and embedded in SlowFade antifade mounting medium (S2828, Thermo Fisher Scientific). Retinal images were taken using a fluorescence microscope (AxioObserver.Z1, Carl Zeiss Microscopy, Jena, Germany) with image software (AxioVision 4.6.3.0, Carl Zeiss Microscopy). Retinal neovascularization was analyzed with the SWIFT_NV macro plugin in ImageJ (Connor et al., 2009).

2.3. Laser-induced Choroidal Neovascularization

The mouse model of laser-induced CNV was used as reported(Poor et al., 2014; Gong et al., 2015). Laser photocoagulation was induced using an image-guided laser system (Micron IV, Phoenix Research Laboratories, Pleasanton, CA) in mice ages 6–8 weeks. Four laser burns at equal distance from the optic nerve head were generated in each eye by a green Argon laser pulse with a wavelength of 532 nm, a fixed diameter of 50 μm, duration of 70 ms, and power level of 240 mW. Eyes were enucleated 7 days after laser photocoagulation and fixed with 4% paraformaldehyde in PBS for 1 h at room temperature. The posterior eye cups consisting of the retinal pigment epithelium/choroid/sclera were dissected and permeabilized with 0.1% Triton X-100 (×100, Thermo Fisher Scientific) in PBS for 1 h at room temperature. The CNV lesions were stained overnight with isolectin GS-IB_4 (10 μg/ml) at room temperature. After washing with PBS, the posterior eye cups were mounted with the scleral side down. Fluorescent images were taken and the areas of lesions were quantified in a masked fashion.

2.4. LC/MS/MS Oxylipid Analysis

Plasma levels of CYP2C8 products from ω-3 and ω-6 LCPUFAs were determined by liquid chromatography tandem mass spectroscopy (LC/MS/MS) after liquid/liquid extraction with ethyl acetate as previously described (Edin et al., 2011; Shao et al., 2014). Online liquid chromatography of extracted samples was performed with an Agilent 1200 Series capillary high performance liquid chromatography (Agilent Technologies, Santa Clara, CA). Separation was achieved using a Phenomenex Luna column (5 m, 150 × 1 mm, Phenomenex, Torrance, CA). Analysis was performed on an MDS Sciex API 3000 equipped with a TurboIonSpray source (Applied Biosystems, Foster City, CA).

2.5. Aortic Ring Assay

Aortae from 3 to 8 week old C57BL/6 J mice were dissected and cut into ~1 mm thick rings(Baker et al., 2012), embedded into growth factor reduced Matrigel (354230, Corning, Corning, New York), and grown in complete classic medium (4Z0-500, Cell Systems, Kirkland, WA) supplemented with CultureBoost (4CB-500, Cell Systems) and Penicillin-Streptomycin (Thermo Fisher) at 37 °C with 5% CO_2. Fenofibric acid (10 μM, 90,568, Sigma-Aldrich), DHA (30 μM, 90310, Cayman Chemical, Ann Arbor, Michigan) or 19,20-EDP (1 μM, 10175, Cayman Chemical) was added to the culture medium 48 h later, and medium was changed every other day. Phase contrast photos of individual explants were taken 6 days after plating and the sprouting area was quantified with ImageJ with a semi-automated macro plugin for quantification of vessel sprouts.

2.6. Choroidal Sprouting Assay

Retinal pigment epithelium/choroid/sclera complex (also referred to as "choroid explant") from 3 week old C57BL/6 J mice was dissected and cut into approximately 1 mm × 1 mm pieces (Shao et al., 2013). The choroid explants were embedded into growth factor reduced Matrigel, cultured and imaged with similar methods used for the aortic ring assay described above.

2.7. Tubule Formation Assay

Human retinal microvascular endothelial cells (HRMECs, ACBRI 181, Cell system) were cultured in endothelial cell growth medium (EGM-2 MV, cc-3202, Lonza, Basel, Switzerland) and used from passage 5 to 8. Cells were seeded onto plates pre-coated with growth factor reduced Matrigel at a density of 2×10^5 cells/ml, and incubated in EGM-2 MV supplemented with fenofibric acid (10 μM), 19,20-EDP (1 μM), DHA (30 μM) or corresponding vehicle controls at 37 °C with 5% CO_2 for 6 h. Phase contrast photos were taken, and the tubule formation was analyzed with Angiogenesis Analyzer for ImageJ.

2.8. Wound Healing Assay

HRMEC were grown to confluence on plates pre-coated with gelatin (0.5 μg/ml, G9391, Sigma-Aldrich). After treatment with mitomycin C (10 μg/ml, Sigma-Aldrich) for 20 min at 37 °C, monolayers were washed, scratched with a pipet tip and incubated in EGM-2 MV at 37 °C for 24 h. Phase contrast photos were taken, and cell migration was quantified by measuring the width of the cell-free zone (distance between the edges of the injured monolayer) at 5 distinct positions (Gong et al., 2013; He et al., 2016). All assays were performed in triplicate.

2.9. Qualitative Real-time Polymerase Chain Reaction

Total RNA was extracted from retinas or HRMECs using RNeasy Kit (74106, Qiagen, Hilden, Germany), and reverse transcribed using random hexamers and SuperScript III Reverse Transcriptase (Thermo Fisher) according to the manufacturer's instructions(Yang et al., 2011; Yang et al., 2013). Quantitative analysis of gene expression was determined using an ABI Prism 7700 Sequence Detection System (Applied BioSystems) and the SYBR Green Master Mix kit (KK4600, Kapa Biosystems, Wilmington, MA)(He et al., 2014) with primers listed below: *CYP2C8* (F: 5′-TGTGGTCCTGGTGCTGTG, R: 5′-ATATTGGGGAATT GCCTCTT), *Acox1* (F: 5′- GAGCAGCAGGAGCGTTTCTT, R: 5′- CAGGACTA TCGCATGATTGGAAG), *Pdk4* (F: 5′- ACAGACATCATAATGTGGTCCCT, R: 5′- GGTCGATACTTCCAATGTGGC), *ACOX1* (F: 5′- ACTCGCAGCCAGCGTTA TG, R: 5′- AGGGTCAGCGATGCCAAAC), PDK4 (F: 5′-GGAGCATTTCTCGCG CTACA, R: 5′-ACAGGCAATTCTTGTCGCAAA), and *Cyclophilin A* (F: 5′-AGG TGGAGAGCACCAAGACAGA, R: 5′-TGCCGGAGTCGACAATGAT). Each target gene cDNA copy number was normalized to the housekeeping gene *Cyclophilin A* using comparative CT (ΔΔCT) method and related to control group.

2.10. Statistical Analysis

Data are presented as mean ± standard error of the mean (SEM). Student's *t*-test was used to compare between 2 groups of samples. For multiple comparisons with additional interventions, two-way ANOVA followed by Tukey's post hoc test was performed using Prism 6 (Graph-Pad, San Diego, CA). The criterion for significance was set at a probability of ≤0.05.

3. Results

3.1. Fenofibrate Reduced Ocular Neovascularization via a PPARα-independent Pathway

To determine if fenofibrate suppressed pathological choroidal and retinal angiogenesis through PPARα alone, both wild-type C57BL/6 and *Pparα* knockout mice were orally gavaged with fenofibrate at 100 μg/g/day or corn oil as vehicle control, and subjected to both OIR and laser-induced CNV. Fenofibrate inhibited retinal neovascularization by 33% ($P = 5.0 \times 10^{-10}$) and CNV by 40% ($P = 1.9 \times 10^{-7}$) in wild-type mice. In *Pparα* knockout mice daily intake of fenofibrate inhibited retinal and choroidal neovascularization by 18% ($P = 0.027$) and 25% ($P = 3.5 \times 10^{-8}$) respectively (Fig. 1a–d), suggesting that in addition to the PPARα pathway, other pathways are involved in the regulation of pathological ocular angiogenesis by fenofibrate. The mRNA levels of two PPARα target genes, *Acox1* and *Pdk4*, were not induced by fenofibrate in the *Pparα* knockout retina, suggesting that fenofibrate did not act through PPARα activation (Fig. 1e&f). These results suggested that fenofibrate suppressed pathological ocular angiogenesis through PPARα-independent as well as PPARα-dependent pathways.

3.2. Fenofibrate Suppressed Ocular Neovascularization via CYP2C8 Inhibition

To determine if fenofibrate suppressed choroidal and retinal neovascularization via CYP2C8 inhibition we used a low dose to primarily inhibit CYP2C activity with minimal PPARα activation (Fig. 2a). To determine the dose at which fenofibrate mainly functions through the CYP2C pathway, *Tie2*-driven human *CYP2C8* overexpressing transgenic mice and their wild-type littermates were orally gavaged with fenofibrate at several low doses. We found that 10 μg/g/day, 1/10 of the standard human dose, decreased the plasma levels of the DHA-derived CYP2C8 product, 19,20-EDP, by 40% ($P = 0.018$) in wild-type and 24% ($P = 0.019$) in *CYP2C8* overexpressing mice (Fig. 2b), but had no effect on CYP2C expression or on mRNA levels of PPARα target genes *Acox1* and *Pdk4* (Fig. 2c–f). The levels of the COX and LOX metabolites, prostaglandin E2 and 5-hydroxyeicosatetraenoic acid respectively, were unchanged suggesting no effect on the COX and LOX metabolizing pathways (Supplemental Table 1). Daily intake of fenofibrate at this low

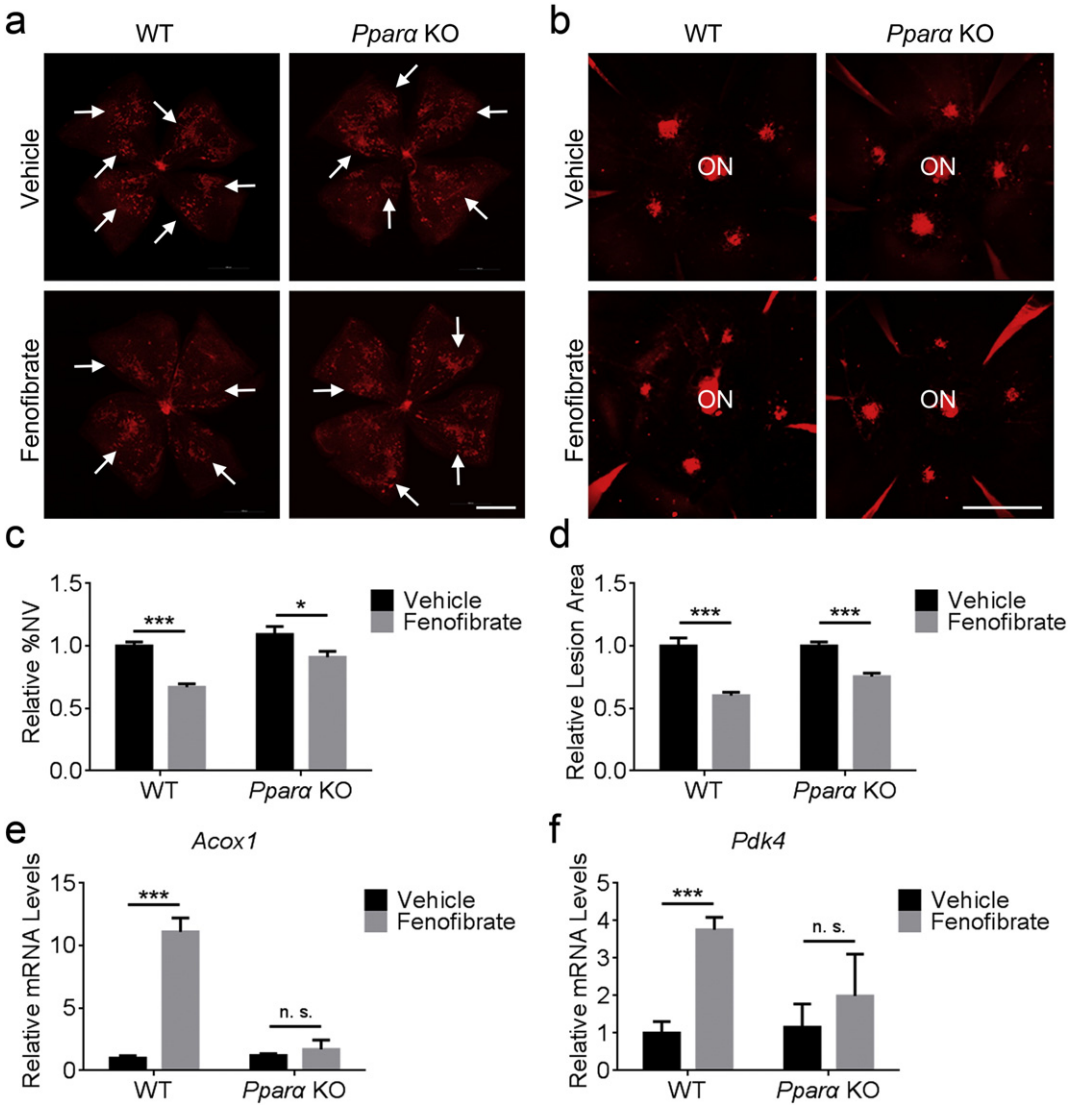

Fig. 1. Fenofibrate suppressed retinal and choridal neovascularization in *Pparα* knockout mice. Wild-type (WT) C57BL/6 and *Pparα* knockout (KO) mice subjected to OIR (**a**, scale bar, 1 mm) or laser-induced CNV (**b**, scale bar, 500 μm; ON, optic nerve) were orally gavaged with fenofibrate (100 μg/g/day) or corn oil as vehicle control from P12 to P16 for OIR or for 7 days after laser photocoagulation. Retinal and choroidal whole-mount vessels were stained with isolectin GS-IB_4 at P17 or 7 days after laser photocoagulation respectively. Fenofibrate reduced retinal (**c**, $n = 10$ mice/group) neovascularization (NV, white arrows) and laser-induced CNV lesion area (**d**, $n = 17$–23 mice/group) in both WT and *Pparα* KO mice. Retinal mRNA levels of *Acox1* (**e**) and *Pdk4* (**f**) were increased in WT and *Pparα* KO mice, normalized to *cyclophilin A* and related to WT vehicle control group. $n = 6$ mice/group. * $P < 0.05$; *** $P < 0.001$; n. s., not significant.

dose (10 μg/g/day) inhibited retinal and choroidal neovascularization induced by CYP2C8 overexpression by 29% ($P = 0.021$) and 36% ($P = 1.2 \times 10^{-9}$) respectively (Fig. 3). These results confirmed that fenofibrate suppressed pathological ocular angiogenesis through a PPARα-independent pathway implicated to be CYP2C8 inhibition.

3.3. Fenofibrate Enhanced the Protective Effects of ω-3 LCPUFAs on Ocular Neovascularization

To test the hypothesis that fenofibrate, as a potent inhibitor of CYP2C, increases the protective effects of ω-3 LCPUFAs on pathological ocular angiogenesis, C57BL/6 mice on a defined isocaloric diet enriched with either ω-6 or ω-3 LCPUFAs were orally gavaged with fenofibrate or vehicle control and P7 pups subjected to OIR and 6–8 week old mice subjected to laser-induced CNV. OIR pups of mothers fed with ω-3 versus ω-6 LCPUFA enriched diets reduced retinal neovascularization at P17 by 25% ($P = 0.023$) (Fig. 4a,b). Laser-induced CNV lesion areas were reduced by 24% ($P = 2.3 \times 10^{-4}$) at 7 days after laser photocoagulation in mice fed with a ω-3 versus ω-6 LCPUFA diet. Fenofibrate increased the protective effect of ω-3 LCPUFAs on retinal and choroidal neovascularization by 12% ($P = 0.031$) and 23% ($P = 2.2 \times 10^{-7}$) respectively (Fig. 4c&d). Fenofibrate-treated animals in the ω-6 LCPUFA dietary group showed similar effects as animals in the ω-3 LCPUFA dietary group that were not treated with fenofibrate. These results indicated that fenofibrate enhanced ω-3 LCPUFA protection on retinal and choroidal neovascularization.

3.4. 19,20-EDP but not DHA Reversed Inhibition of ex vivo Angiogenesis by Fenofibric Acid

To examine whether fenofibrate reduced neovascularization via CYP2C inhibition and decreased levels of its DHA metabolites, we investigated the effects of fenofibric acid, the biologically active derivative of fenofibrate, on angiogenesis in ex vivo tissue explants. In an aortic ring angiogenic assay, fenofibric acid inhibited aortic ring sprouting by 41% ($P = 0.0057$), and the CYP2C DHA product, 19,20-EDP, reversed

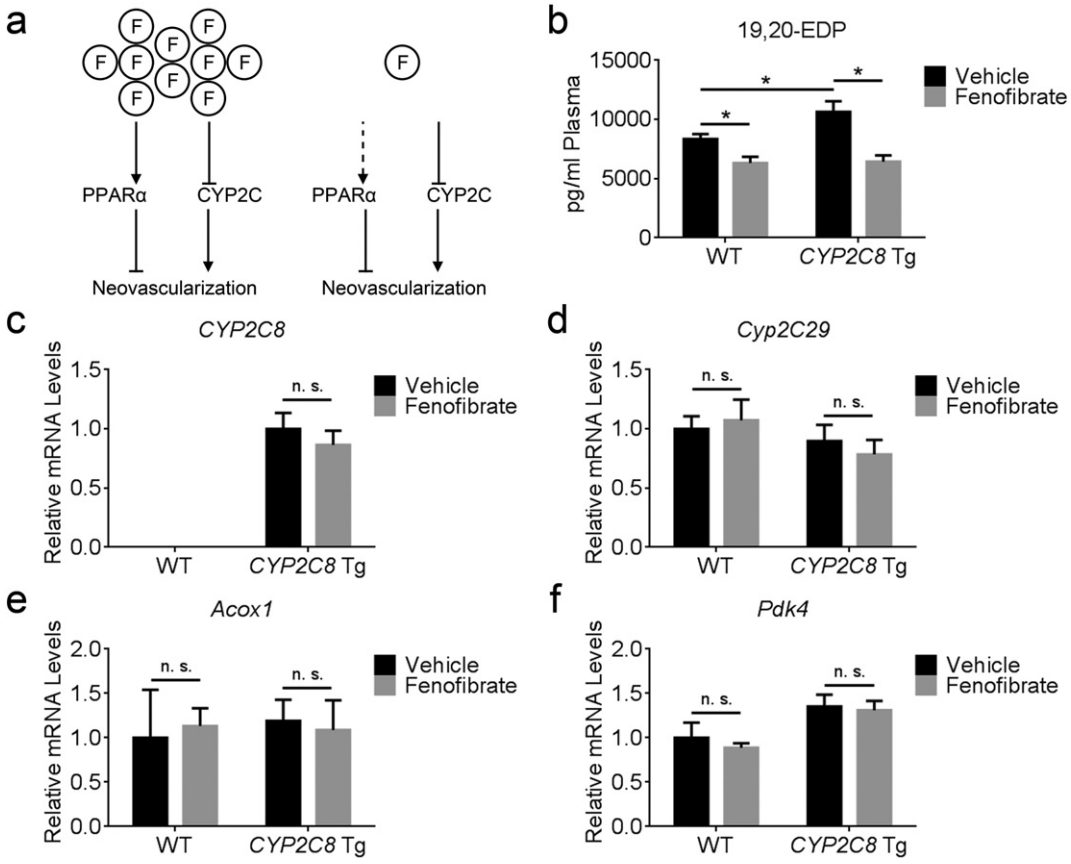

Fig. 2. Fenofibrate at a low dose inhibited CYP2C8 activity without PPARα activation. (**a**) Fenofibrate (F) has different effects on PPARα and CYP2C pathways at different doses due to their different affinity to fenofibrate. (**b**) *Tie2*-driven *CYP2C8* transgenic (Tg) and wild-type (WT) littermate mice were orally gavaged with fenofibrate (10 μg/g/day) or 10% DMSO as vehicle control for 5 days. Fenofibrate at the low dose reversed the induction of 19,20-EDP plasma levels in *CYP2C8* Tg mice. n = 10 mice/group, * $P < 0.05$. The mRNA levels of *CYP2C8* (**c**), *Cyp2C29* (**d**), *Acox1* (**e**) and *Pdk4* (**f**) were not affected by fenofibrate at the low dose in both the WT and *CYP2C8* Tg retina. n = 6 mice/group, n. s., not significant.

fenofibric acid suppression of angiogenesis by 42% ($P = 0.0069$) (Fig. 4a,c). In the choroidal sprouting assay, similar results were observed. Fenofibric acid decreased the sprouting area from choroidal explants by 51% ($P = 0.0053$), and 19,20-EDP reversed its inhibitory effects by 37% ($P = 0.0035$) (Fig. 4b,d). The addition of DHA, the precursor of not only CYP2C-derived 19,20-EDP but also of COX and LOX derived *anti*-angiogenic metabolites, further potentiated the anti-angiogenic effect of fenofibrate acid on the aortic ring and choroidal explant sprouting (Fig. 5). Co-treatment with fenofibric acid and DHA led to 78% ($P = 2.4 \times 10^{-4}$) and 41% ($P = 0.031$) reduction in sprouting area from aorta and choroid versus 62% ($P = 0.0049$) and 32% ($P = 0.030$) reduction with fenofibric acid alone and 43% ($P = 9.6 \times 10^{-5}$) and 13% ($P = 0.042$) reduction with DHA alone (Fig. 6). These data suggested that fenofibric acid inhibited angiogenesis ex vivo via CYP2C inhibition resulting in decreased levels of CYP2C DHA pro-angiogenic products including 19,20-EDP.

3.5. 19,20-EDP but not DHA Reversed the Inhibition of Endothelial Cell Functions by Fenofibric Acid

To clarify the specific cell type and behavior of the *anti*-angiogenic effects of fenofibric acid in ocular neovascularization, we examined fenofibrate's effects on endothelial cell tubule formation and migration in vitro using HRMECs. Fenofibric acid suppressed tubule formation compared with cells treated with vehicle control, resulting in fewer tube junctions (Fig. 7a,c). In addition, fenofibric acid suppressed HRMEC migration in a wound healing scratch assay (Fig. 7b,d). 19,20-EDP rescued the suppression of HRMEC tubule formation and migration by fenofibric acid (Fig. 7). However, DHA did not reverse the inhibition of endothelial cell tubule formation or migration by fenofibric acid, but further augmented the inhibitory effects of fenofibric acid (Fig. 8). These results indicated that fenofibric acid impaired endothelial cell functions via CYP2C inhibition and the DHA metabolites of CYP2C could reverse its inhibition.

4. Discussion

Fenofibrate has been found in interventional clinical studies (FIELD, ACCORD and MacuFen) to reduce the rates of progression of sight-threatening diabetic retinopathy and the volume of macular edema (Keech et al., 2007; Group et al., 2010; Massin et al., 2014). The *anti*-retinopathy effects appear to be independent of a fenofibrate-driven activation of PPARα and subsequent lipid lowering effect(Keech et al., 2007; Wong et al., 2012; Yu and Lyons, 2013). We found that fenofibrate inhibited neovascularization in *Pparα* knockout mice through inhibition of CYP2C to decrease CYP2C-derived ω-3 LCPUFA pro-angiogenic metabolites as well as via PPARα activation.

The fenofibrate dose that we used in mice in this study (100 mg/kg/day) (Hu et al., 2013) is comparable to that used in the FIELD and ACCORD clinical trials for lipid lowering effects and induced the expression of PPARα target genes, such as Acox1 and Pdk4, in the retina. Because the index of human equivalent dose to mice is 0.081 and absorption after oral gavage in rodents is 25–50%(Reagan-Shaw et al., 2008), the corresponding human dose is 2–4 mg/kg/day which is comparable to the dose used in the FIELD (200 mg/60 kg/day or ~3.3 mg/kg/day) and the ACCORD (160 mg/60 kg/day or ~2.7 mg/kg/day) studies (Keech et al., 2005; Chew et al., 2007), suggesting that PPARα activation might contribute to the beneficial effects of fenofibrate on retinopathy

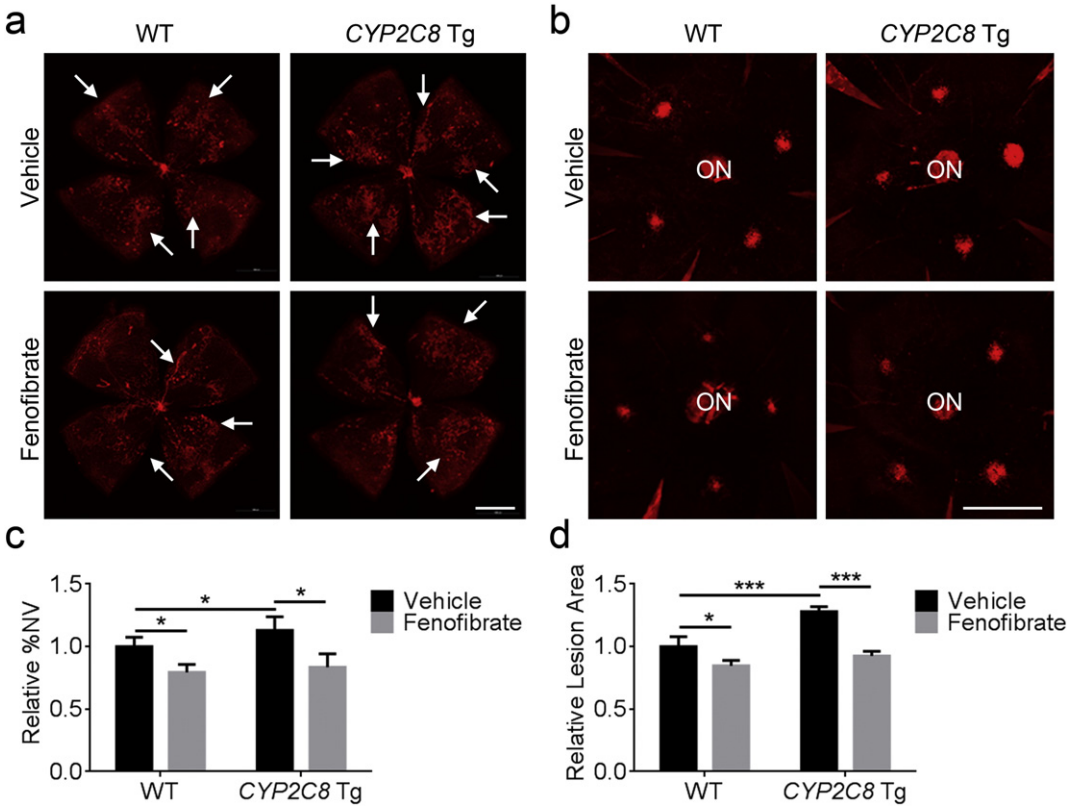

Fig. 3. Fenofibrate at a low dose suppressed both retinal and choroidal neovascularization in mice overexpressing *CYP2C8*. *Tie2*-driven *CYP2C8* overexpression transgenic (Tg) and wild-type (WT) littermate mice were subjected to OIR (**a**, scale bar, 1 mm) or laser-induced CNV (**b**, scale bar, 500 μm; ON, optic nerve). The mice were orally gavaged with fenofibrate (10 μg/g/day) or 10% DMSO as vehicle control from P12 to P16 for OIR or for 7 days after laser photocoagulation respectively. Retinal and choroidal whole-mount vessels were stained with isolectin GS-IB4 at P17 or 7 days after laser photocoagulation respectively. Fenofibrate at the lower dose suppressed the induction of retinal (**c**) neovascularization (NV, white arrows) and laser-induced CNV lesion area (**d**) in *CYP2C8* Tg mice. n = 10–12 mice/group. * $P < 0.05$; *** $P < 0.001$.

progression in patients with type 2 diabetes. The affinity of fenofibrate to CYP2C is >10 times higher than to PPARα(Walsky et al., 2005; Schoonjans et al., 1996). We found that oral gavage of fenofibrate at one tenth the dose (10 mg/kg/day) in mice decreased the plasma levels of LCPUFA products metabolized by CYP2C including 19,20-EDP and 14,15-EET, but had no measurable effect on PPARα target gene mRNA expression in the retina, suggesting that in humans, inhibition of CYP2C activity by fenofibrate might also contribute to its protective effects on pathological ocular angiogenesis in these two large-scale clinical trials.

Fenofibrate is pharmacologically inactive and with ingestion undergoes rapid hydrolysis of the ester bond to form the active metabolite fenofibric acid (Wang et al., 2014). Fenofibrate inhibits angiogenesis in vivo and in vitro by decreasing basic fibroblast growth factor-induced Akt activation and cytokine-induced vascular cell adhesion molecule 1 expression in endothelial cells through PPARα activation (Varet et al., 2003; Marx et al., 1999). Fenofibrate also affects retinal endothelial cells in a PPARα-independent manner. For example, fenofibrate regulates the survival of HRMECs, but pretreatment with the PPARα antagonist MK 886 fails to alter this effect. Another selective agonist of PPARα, WY-14643, has no discernible effect on HRMEC survival (Kim et al., 2007). We also found that another PPARα antagonist GW6471 failed to alter the inhibitory effects of fenofibric acid on angiogenesis ex vivo and in vitro (Supplemental Fig. 1 & 2). In human umbilical vein endothelial cells, fenofibrate increases 5′ adenosine monophosphate-activated protein kinase phosphorylation, but neither PPARα activator bezafibrate nor WY-14,643 has the same effect (Murakami et al., 2006). Studies of PPARα-independent mechanisms of action of fenofibrate and identification of the master regulators of PPARα-independent effects are still limited. Our results suggested CYP2C as a potential PPARα-independent mediator of fenofibrate action in endothelial cells.

CYP2C comprises a major group of CYP mixed-function epoxygenases involved in the oxidation of both xenobiotic and endogenous compounds (Edin et al., 2011). Many drugs, including fenofibrate, are metabolized by CYP2C enzymes (Walsky et al., 2005). In addition to being a CYP2C substrate, fenofibrate is also reported to regulate the expression of some CYP2C isoforms in the kidney (Muller et al., 2004). CYP2C8, together with CYP2C9, is one of the most abundant CYP2C enzymes in human tissues and their epoxygenase activity modulates both physiological and pathological angiogenesis (Tsao et al., 2001). CYP2C8 homologues in mice, such as Cyp2C29 and Cyp2C55, are expressed in macrophages and endothelial cells in the eye, and they are induced by OIR (Nelson et al., 2004; Shao et al., 2014). Fenofibrate is identified by in vitro screening as a potent suppressor of CYP2C8, as well as CYP2C9(Walsky et al., 2005). In our studies, fenofibrate reduced retinal and choroidal neovascularization not only in *Tie2*-driven human *CYP2C8* transgenic mice but also in wild-type mice, which suggested that fenofibrate inhibited not only exogenous human CYP2C8 but also endogenous mouse Cyp2C activity. We also showed that fenofibrate had no effect on *CYP2C8* and *Cyp2C29* mRNA levels, indicating that its protective effects on ocular neovascularization were mediated by CYP2C activity but not expression.

Dietary intake of ω-3 versus ω-6 LCPUFAs reduces pathological ocular angiogenesis (Connor et al., 2007; Koto et al., 2007; Moghaddam-Taaheri et al., 2011). The ω-3 LCPUFA, DHA, inhibits angiogenesis ex vivo and endothelial functions in vitro, which is consistent with previous publications and likely related to its metabolites produced through cyclooxygenase and lipoxygenase, rather than through CYP pathways (Sapieha et al., 2011; Szymczak et al., 2008; Gong et al., 2016). The different effects reported on CNV of an exogenously delivered single ω-3 LCPUFA CYP

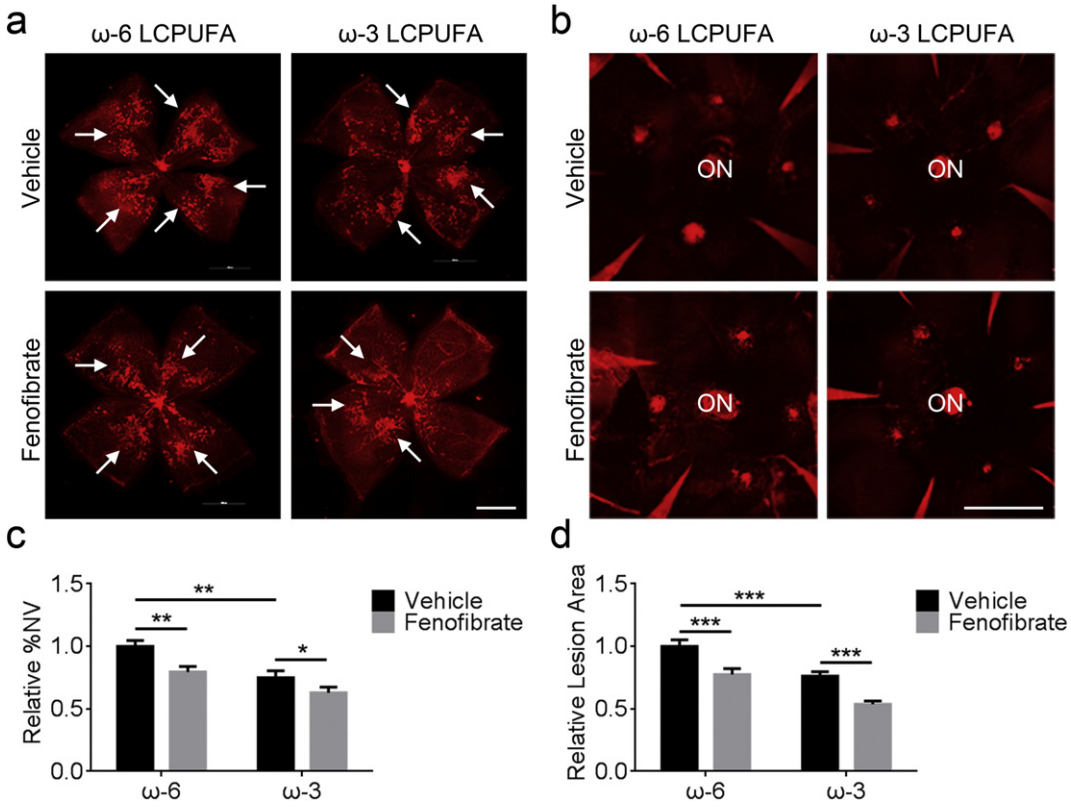

Fig. 4. Fenofibrate augmented the protective effects of ω-3 LCPUFAs against retinal and choridal neovascularization. Wild-type C57BL/6 mice fed with a ω-6 or ω-3 LCPUFA enriched diet were subjected to OIR (**a**, scale bar, 1 mm) or laser-induced CNV (**b**, scale bar, 500 μm; ON, optic nerve). The mice were orally gavaged with fenofibrate (100 μg/g/day) or corn oil as vehicle control from P12 to P16 for OIR or for 7 days after laser photocoagulation. Retinal and choroidal whole-mount vessels were stained with isolectin GS-IB_4 at P17 or 7 days after laser photocoagulation respectively. Fenofibrate augmented the protective effects of ω-3 LCPUFAs on retinal (**c**) neovascularization (NV, white arrows) and laser-induced CNV lesion area (**d**). n = 10 mice/group. * $P < 0.05$; ** $P < 0.01$; *** $P < 0.001$.

metabolite might result from a different plasma concentration due to exogenous administration rather than an evaluation of the sum total of all metabolites after inhibition of CYP2C activity(Yanai et al., 2014; Gong et al., 2016). DHA supplementation did not reverse the angiogenesis inhibitory effects of fenofibrate, but further increased the suppression of angiogenesis, suggesting that DHA on balance was metabolized by other enzymes into *anti*-angiogenic metabolites and that fenofibrate functioned downstream of DHA. In contrast to the modest increase in anti-angiogenic effects of DHA on the inhibition of angiogenesis with fenofibrate, addition of CYP2C products derived from DHA, such as 19,20-EDP, reversed the inhibitory effects of fenofibrate on angiogenesis ex vivo and endothelial cell functions in vitro, suggesting that fenofibrate functioned upstream of CYP2C products. Our results suggested that inhibition of CYP2C activity by fenofibrate augmented the protective effect of ω-3 LCPUFAs on pathological ocular angiogenesis.

Fenofibrate reversed the induction of retinal and choroidal neovascularization in CYP2C8 overexpressing mice fed either a ω-3 or ω-6 LCPUFA enriched diet, suggesting that CYP2C products derived from both ω-3 and ω-6 LCPUFAs were pro-angiogenic in the retina and choroid. A previous study shows that 19,20-EDP inhibits tumor growth and human umbilical vein endothelial cell functions in vitro (Zhang et al., 2013). The different expression pattern of growth factors and metabolic enzymes in the retina and in tumor might contribute to the different effects of the CYP2C metabolite observed, indicating a tissue-specific role of 19,20-EDP. Knowledge on the molecular mechanism or regulation of angiogenesis and endothelial cell behaviors by CYP2C metabolites, such as EDPs and EETs, is still limited. Previous studies suggest that 11,12-EET induces angiogenesis in human umbilical vein endothelial cells through the phosphatidylinositol-3-OH kinase pathway mediating phosphorylation of FOXO factors which cause decreased expression of the cyclin dependent kinase inhibitor $p27^{Kip1}$, and that 14,15-EET promotes angiogenesis in a mouse wound healing model through VEGF induction (Potente et al., 2003; Sander et al., 2013). A recent study indicates that 11,12-EET promotes hematopoietic stem and progenitor cell specification by increasing activator protein 1 and runx1 transcription through the phosphatidylinositol-3-OH kinase pathway(Li et al., 2015), which has also been implicated in advanced AMD by our previous work (SanGiovanni et al., 2009b). More research on the direct target and downstream pathways of CYP2C metabolites is needed.

In summary we found that fenofibrate inhibited pathological ocular angiogenesis by suppressing CYP2C activity that led to decreased levels of CYP2C pro-angiogenic products from both ω-6 and ω-3 LCPUFAs. Dietary intake of ω-3 LCPUFAs helped prevent retinal and choroidal neovascularization and CYP2C inhibition by fenofibrate enhanced the protective effects of ω-3 LCPUFAs against pathological angiogenesis in the eye. Combination therapy of dietary ω-3 LCPUFA supplementation with fenofibrate may be a promising approach to prevent incidence or progression of abnormal retinal and choroidal neovascularization.

Conflicts of Interest

The authors declare no conflicts of interest.

Funding Sources

This work was supported by the National Institutes of Health/National Eye Institute (R01 EY024864, EY017017, and P01 HD18655), Lowy Medical Research Institute (#84134), European Commission FP7 PREVENT-ROP project (305485 LEHS), Knights Templar Eye Foundation

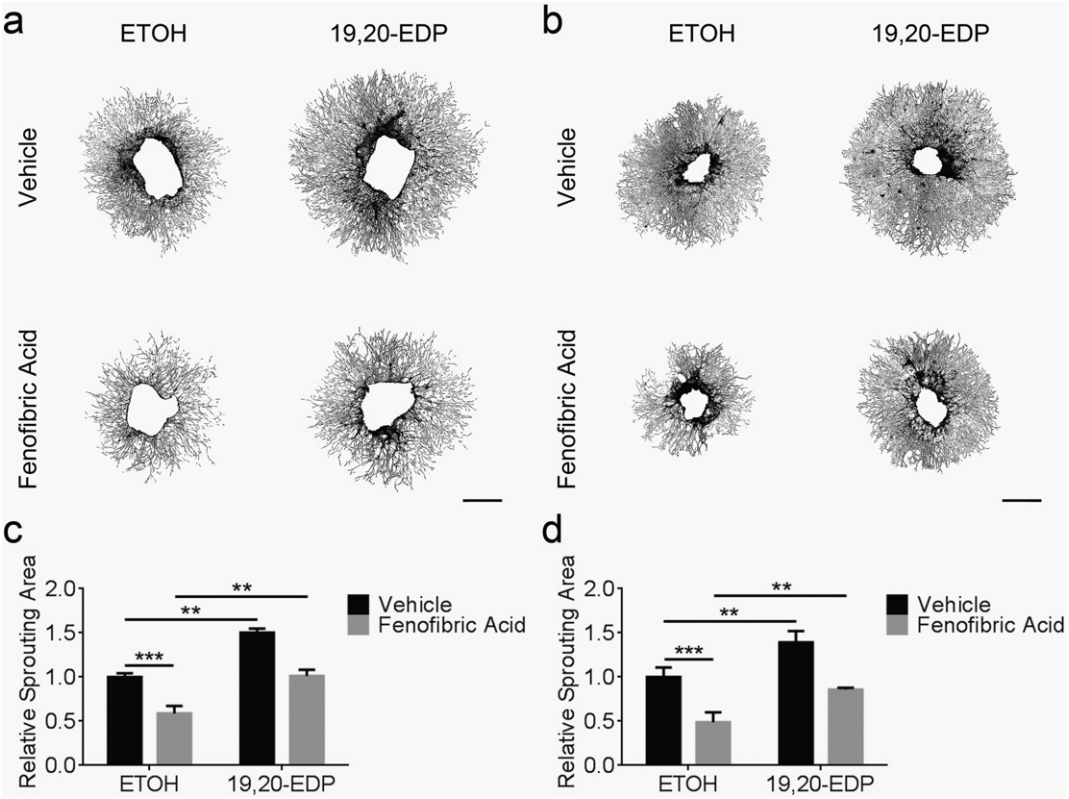

Fig. 5. 19,20-EDP reversed the inhibition of angiogenesis ex vivo by fenofibric acid. Aortic rings (**a**) and choroidal explants (**b**) were treated with fenofibric acid (20 μM) or 1% DMSO as vehicle control, and 19,20-EDP (1 μM) or ethanol (ETOH) as vehicle control for 6 days after tissue planting. Scale bar, 1 mm. 19,20-EDP reversed the inhibition of aortic ring (**c**) and choroidal (**d**) sprouting by fenofibric acid. $n = 6$. ** $P < 0.01$.

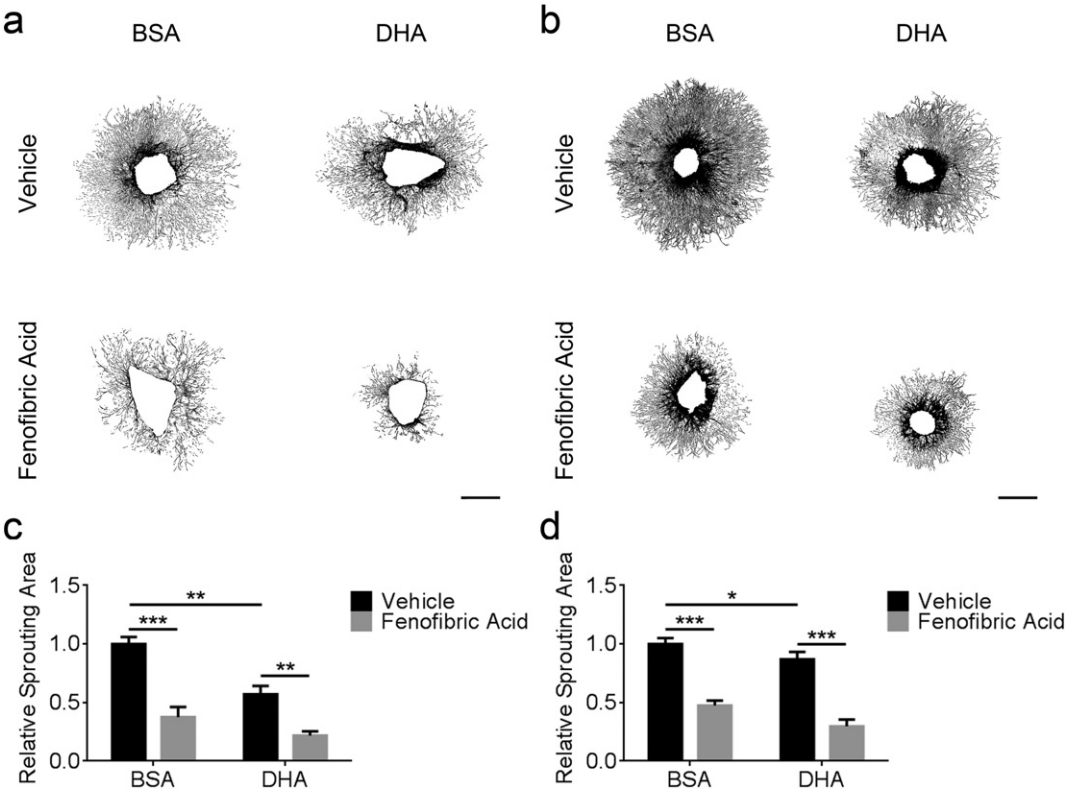

Fig. 6. DHA enhanced the inhibition of angiogenesis ex vivo by fenofibric acid. Aortic rings (**a**) and choroidal explants (**b**) were treated with fenofibric acid (20 μM) or 1% DMSO as vehicle control, and DHA (30 μM) or 10% BSA as vehicle control for 6 days after tissue planting. Scale bar, 1 mm. DHA enhanced the inhibition of aortic ring (**c**) and choroidal (**d**) sprouting by fenofibric acid. n = 6. * $P < 0.05$; ** $P < 0.01$; *** $P < 0.001$.

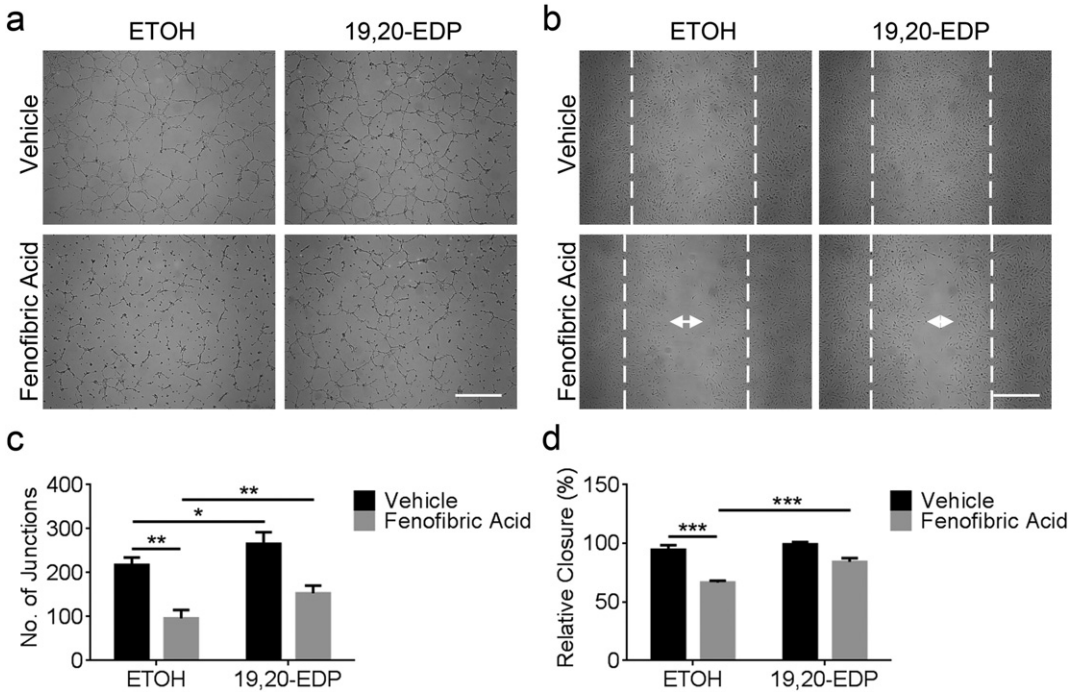

Fig. 7. 19,20-EDP reversed the inhibition of endothelial cell tubule formation and migration by fenofibric acid. Representative photos of HRMEC tubule formation (**a**) and scratch wound healing assays (**b**) treated with fenofibric acid (20 μM) or 1% DMSO as vehicle control, and 19,20-EDP (1 μM) or ETOH as vehicle control. Scale bar, 500 μm. Dashed lines indicate scratched area and white arrows indicate cell-free zone 24 h later. 19,20-EDP reversed the inhibition of endothelial cell tubule formation (**c**) and migration (**d**) by fenofibric acid. n = 6. * $P < 0.05$; ** $P < 0.01$; *** $P < 0.001$.

(#78072) and Bernadotte Foundation (BCH-ZF), Republic of China Ministry of Science and Technology Postdoctoral Research Abroad Program (104-2917-I-564-026 CHL), and in part by National Institutes of Health/National Institute of Environmental Health Sciences (Z01 025034 DCZ).

Author Contributions

Y.G., Z.S., D.C.Z., A.H., and L.E.H.S. conceived the study, Y.G., Z.S., Z.F., M.L.E., Y.S., R.L., Z.W., C.H.L., S.B.B., S.S.M., and F.B.L. conducted the

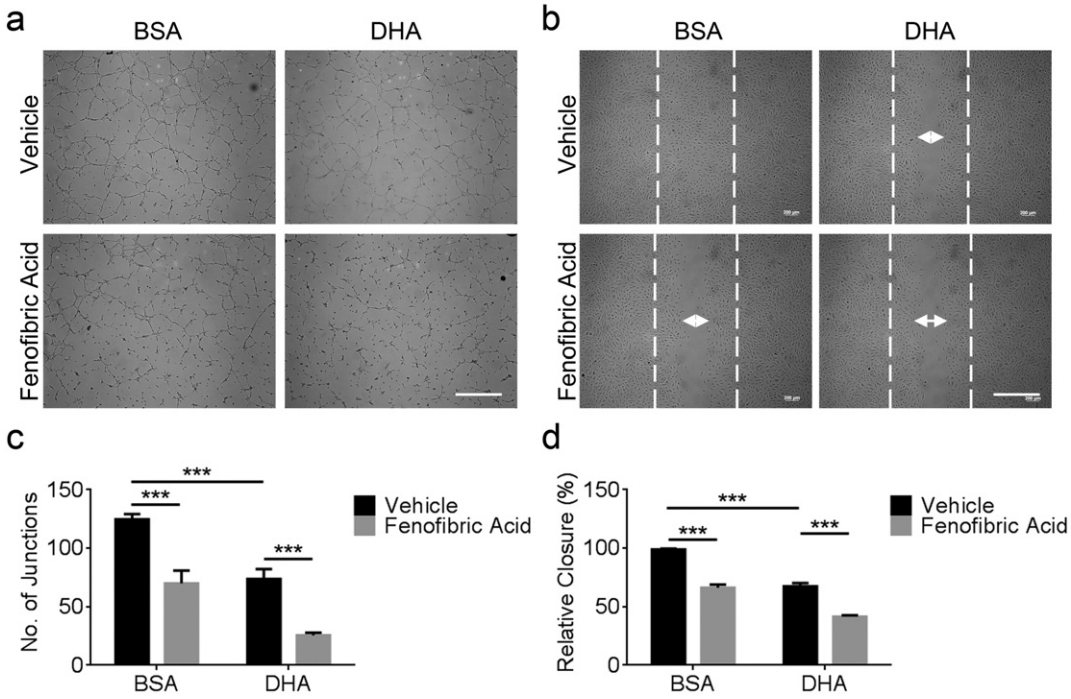

Fig. 8. DHA enhanced the inhibition of human endothelial cell tubule formation and migration by fenofibric acid. Representative photos of HRMEC tubule formation (**a**) and scratch wound healing assays (**b**) with fenofibric acid treatment (20 μM) or 1% DMSO as vehicle control, and DHA (30 μM) or 10% BSA as vehicle control. Scale bar, 500 μm. Dashed lines indicate scratched area and white arrows indicate cell-free zone 24 h later. DHA enhanced the inhibition of endothelial cell tubule formation (**c**) and migration (**d**) by fenofibric acid. n = 6. *** $P < 0.001$.

experiments, Y.G., M.L.E., J.P.S.G., D.C.Z. and L.E.H.S. analyzed the results. All authors reviewed the manuscript.

Acknowledgments

We thank Drs. Jing Chen and Dipak Panigrahy for helpful discussions, and Dr. Jie Li, Christian G. Hurst, Ricky Z. Cui, Lucy P. Evans, Katherine T. Tian, Thomas W. Fredrick, Nicholas J. Saba, Peyton C. Morss and James D. Loewke for excellent technical support.

Appendix A. Supplementary Data

Supplementary data to this article can be found online at http://dx.doi.org/10.1016/j.ebiom.2016.09.025.

References

Antonetti, D.A., Klein, R., gardner, T.W., 2012. Diabetic retinopathy. N. Engl. J. Med. 366, 1227–1239.

Baker, M., Robinson, S.D., Lechertier, T., Barber, P.R., Tavora, B., D'amico, G., Jones, D.T., Vojnovic, B., Hodivala-Dilke, K., 2012. Use of the mouse aortic ring assay to study angiogenesis. Nat. Protoc. 7, 89–104.

Bogdanov, P., Hernandez, C., Corraliza, L., Carvalho, A.R., SIMO, R., 2015. Effect of fenofibrate on retinal neurodegeneration in an experimental model of type 2 diabetes. Acta Diabetol. 52, 113–122.

Cheung, N., Lam, D.S., Wong, T.Y., 2012. Anti-vascular endothelial growth factor treatment for eye diseases. BMJ 344, e2970.

Chew, E.Y., Ambrosius, W.T., Howard, L.T., Greven, C.M., Johnson, S., Danis, R.P., Davis, M.D., Genuth, S., Domanski, M., Group, A.S., 2007. Rationale, design, and methods of the Action to Control Cardiovascular Risk in Diabetes Eye Study (ACCORD-EYE). Am. J. Cardiol. 99, 103i–111i.

Connor, K.M., Sangiovanni, J.P., Lofqvist, C., Aderman, C.M., Chen, J., Higuchi, A., Hong, S., Pravda, E.A., Majchrzak, S., Carper, D., Hellstrom, A., Kang, J.X., Chew, E.Y., Salem, N., Serhan JR., C.N., Smith, L.E., 2007. Increased dietary intake of omega-3-polyunsaturated fatty acids reduces pathological retinal angiogenesis. Nat. Med. 13, 868–873.

Connor, K.M., Krah, N.M., Dennison, R.J., Aderman, C.M., Chen, J., Guerin, K.I., Sapieha, P., Stahl, A., Willett, K.L., Smith, L.E., 2009. Quantification of oxygen-induced retinopathy in the mouse: a model of vessel loss, vessel regrowth and pathological angiogenesis. Nat. Protoc. 4, 1565–1573.

Edin, M.L., Wang, Z., Bradbury, J.A., Graves, J.P., Lih, F.B., Degraff, L.M., Foley, J.F., Torphy, R., Ronnekleiv, O.K., Tomer, K.B., Lee, C.R., Zeldin, D.C., 2011. Endothelial expression of human cytochrome P450 epoxygenase CYP2C8 increases susceptibility to ischemia-reperfusion injury in isolated mouse heart. FASEB J. 25, 3436–3447.

Fu, Z., Gong, Y., Lofqvist, C., Hellstrom, A., Smith, L.E., 2016. Review: adiponectin in retinopathy. Biochim. Biophys. Acta 1862, 1392–1400.

Gibson, D.M., 2012. Diabetic retinopathy and age-related macular degeneration in the U.S. Am. J. Prev. Med. 43, 48–54.

Gong, Y., Yang, X., He, Q., Gower, L., Prudovsky, I., Vary, C.P., Brooks, P.C., Friesel, R.E., 2013. Sprouty4 regulates endothelial cell migration via modulating integrin beta3 stability through c-Src. Angiogenesis 16, 861–875.

Gong, Y., Li, J., Sun, Y., Fu, Z., Liu, C.H., Evans, L., Tian, K., Saba, N., Fredrick, T., Morss, P., Chen, J., smith, L.E., 2015. Optimization of an image-guided laser-induced choroidal neovascularization model in mice. PLoS One 10, e0132643.

Gong, Y., Fu, Z., Edin, M.L., Liu, C.H., Wang, Z., Shao, Z., Fredrick, T.W., Saba, N.J., Morss, P.C., Burnim, S.B., Meng, S.S., Lih, F.B., Lee, K.S., Moran, E.P., Sangiovanni, J.P., Hellstrom, A., Hammock, B.D., Zeldin, D.C., Smith, L.E., 2016. Cytochrome P450 oxidase 2C inhibition adds to omega-3 long-chain polyunsaturated fatty acids protection against retinal and choroidal neovascularization. Arterioscler. Thromb. Vasc. Biol. 36, 1919–1927.

Group, A.S., Group, A.E.S., Chew, E.Y., Ambrosius, W.T., Davis, M.D., Danis, R.P., Gangaputra, S., Greven, C.M., Hubbard, L., ESSER, B.A., Lovato, J.F., Perdue, L.H., Goff, D.C., Cushman JR., W.C., Ginsberg, H.N., Elam, M.B., Genuth, S., Gerstein, H.C., Schubart, U., Fine, L.J., 2010. Effects of medical therapies on retinopathy progression in type 2 diabetes. N. Engl. J. Med. 363, 233–244.

He, Q., Yang, X., Gong, Y., Kovalenko, D., Canalis, E., Rosen, C.J., Friesel, R.E., 2014. Deficiency of Sef is associated with increased postnatal cortical bone mass by regulating Runx2 activity. J. Bone Miner. Res. 29, 1217–1231.

He, Q., Gong, Y., Gower, L., Yang, X., Friesel, R.E., 2016. Sef regulates epithelial-mesenchymal transition in breast cancer cells. J. Cell Biochem.

Hellstrom, A., Smith, L.E., Dammann, O., 2013. Retinopathy of prematurity. Lancet 382, 1445–1457.

Hu, Y., Chen, Y., Ding, L., He, X., Takahashi, Y., Gao, Y., Shen, W., Cheng, R., Chen, Q., Qi, X., Boulton, M.E., Ma, J.X., 2013. Pathogenic role of diabetes-induced PPAR-alpha down-regulation in microvascular dysfunction. Proc. Natl. Acad. Sci. U. S. A. 110, 15401–15406.

Keech, A., Simes, R.J., Barter, P., Best, J., Scott, R., Taskinen, M.R., Forder, P., Pillai, A., Davis, T., Glasziou, P., Drury, P., Kesaniemi, Y.A., Sullivan, D., Hunt, D., Colman, P., D'Emden, M., Whiting, M., Ehnholm, C., Laakso, M., Investigators, F.S., 2005. Effects of long-term fenofibrate therapy on cardiovascular events in 9795 people with type 2 diabetes mellitus (the FIELD study): randomised controlled trial. Lancet 366, 1849–1861.

Keech, A.C., Mitchell, P., Summanen, P.A., O'day, J., Davis, T.M., Moffitt, M.S., Taskinen, M.R., Simes, R.J., Tse, D., Williamson, E., Merrifield, A., Laatikainen, L.T., D'emden, M.C., Crimet, D.C., O'connell, R.L., Colman, P.G., 2007. Effect of fenofibrate on the need for laser treatment for diabetic retinopathy (FIELD study): a randomised controlled trial. Lancet 370, 1687–1697.

Kim, J., Ahn, J.H., Kim, J.H., Yu, Y.S., Kim, H.S., Ha, J., Shinn, S.H., Oh, Y.S., 2007. Fenofibrate regulates retinal endothelial cell survival through the AMPK signal transduction pathway. Exp. Eye Res. 84, 886–893.

Koto, T., Nagai, N., Mochimaru, H., Kurihara, T., Izumi-Nagai, K., Satofuka, S., Shinoda, H., Noda, K., Ozawa, Y., Inoue, M., Tsubota, K., Oike, Y., Ishida, S., 2007. Eicosapentaenoic acid is anti-inflammatory in preventing choroidal neovascularization in mice. Invest. Ophthalmol. Vis. Sci. 48, 4328–4334.

Li, P., Lahvic, J.L., Binder, V., Pugach, E.K., Riley, E.B., Tamplin, O.J., Panigrahy, D., Bowman, T.V., Barrett, F.G., Heffner, G.C., Mckinney-Freeman, S., Schlaeger, T.M., Daley, G.Q., Zeldin, D.C., Zon, L.I., 2015. Epoxyeicosatrienoic acids enhance embryonic haematopoiesis and adult marrow engraftment. Nature 523, 468–471.

Liu, C.H., Sun, Y., Li, J., Gong, Y., Tian, K.T., Evans, L.P., Morss, P.C., Fredrick, T.W., Saba, N.J., Chen, J., 2015. Endothelial microRNA-150 is an intrinsic suppressor of pathologic ocular neovascularization. Proc. Natl. Acad. Sci. U. S. A. 112, 12163–12168.

Marx, N., Sukhova, G.K., Collins, T., Libby, P., Plutzky, J., 1999. PPARalpha activators inhibit cytokine-induced vascular cell adhesion molecule-1 expression in human endothelial cells. Circulation 99, 3125–3131.

Massin, P., Peto, T., Ansquer, J.C., Aubonnet, P., Macu, F.E.N.S.I.F.T., 2014. Effects of fenofibric acid on diabetic macular edema: the MacuFen study. Ophthalmic Epidemiol. 21, 307–317.

Moghaddam-Taaheri, S., Agarwal, M., Amaral, J., Fedorova, I., Agron, E., Salem, N., Chew JR., E., Becerra, S.P., 2011. Effects of docosahexaenoic acid in preventing experimental choroidal neovascularization in rodents. J. Clin. Exp. Ophthalmol. 2.

Moran, E., Ding, L., Wang, Z., Cheng, R., Chen, Q., Moore, R., Takahashi, Y., Ma, J.X., 2014. Protective and antioxidant effects of PPARalpha in the ischemic retina. Invest. Ophthalmol. Vis. Sci. 55, 4568–4576.

Muller, D.N., Theuer, J., Shagdarsuren, E., Kaergel, E., Honeck, H., Park, J.K., Markovic, M., Barbosa-Sicard, E., Dechend, R., Wellner, M., Kirsch, T., Fiebeler, A., Rothe, M., Haller, H., Luft, F.C., Schunck, W.H., 2004. A peroxisome proliferator-activated receptor-alpha activator induces renal CYP2C23 activity and protects from angiotensin II-induced renal injury. Am. J. Pathol. 164, 521–532.

Murakami, H., Murakami, R., Kambe, F., Cao, X., Takahashi, R., Asai, T., Hirai, T., Numaguchi, Y., Okumura, K., Seo, H., Murohara, T., 2006. Fenofibrate activates AMPK and increases eNOS phosphorylation in HUVEC. Biochem. Biophys. Res. Commun. 341, 973–978.

Nelson, D.R., Zeldin, D.C., Hoffman, S.M., Maltais, L.J., Wain, H.M., Nebert, D.W., 2004. Comparison of cytochrome P450 (CYP) genes from the mouse and human genomes, including nomenclature recommendations for genes, pseudogenes and alternative-splice variants. Pharmacogenetics 14, 1–18.

Poor, S.H., Qiu, Y., Fassbender, E.S., Shen, S., Woolfenden, A., Delpero, A., Kim, Y., Buchanan, N., Gebuhr, T.C., Hanks, S.M., Meredith, E.L., Jaffee, B.D., Dryja, T.P., 2014. Reliability of the mouse model of choroidal neovascularization induced by laser photocoagulation. Invest. Ophthalmol. Vis. Sci. 55, 6525–6534.

Potente, M., Fisslthaler, B., Busse, R., Fleming, I., 2003. 11,12-epoxyeicosatrienoic acid-induced inhibition of FOXO factors promotes endothelial proliferation by down-regulating p27Kip1. J. Biol. Chem. 278, 29619–29625.

Reagan-Shaw, S., Nihal, M., Ahmad, N., 2008. Dose translation from animal to human studies revisited. FASEB J. 22, 659–661.

Sander, A.L., Sommer, K., Neumayer, T., Fleming, I., Marzi, I., Barker, J.H., Frank, J., Jakob, H., 2013. Soluble epoxide hydrolase disruption as therapeutic target for wound healing. J. Surg. Res. 182, 362–367.

Sangiovanni, J.P., Chew, E.Y., 2005. The role of omega-3 long-chain polyunsaturated fatty acids in health and disease of the retina. Prog. Retin. Eye Res. 24, 87–138.

Sangiovanni, J.P., Agron, E., Meleth, A.D., Reed, G.F., Sperduto, R.D., Clemons, T.E., Chew, E.Y., 2009a. {omega}-3 long-chain polyunsaturated fatty acid intake and 12-y incidence of neovascular age-related macular degeneration and central geographic atrophy: AREDS report 30, a prospective cohort study from the age-related eye disease study. Am. J. Clin. Nutr. 90, 1601–1607.

Sangiovanni, J.P., Mehta, S., Mehta, S., 2009b. Variation in lipid-associated genes as they relate to risk of advanced age-related macular degeneration. World Rev. Nutr. Diet. 99, 105–158.

Sapieha, P., Stahl, A., Chen, J., Seaward, M.R., Willett, K.L., Krah, N.M., Dennison, R.J., Connor, K.M., Aderman, C.M., Liclican, E., Carughi, A., Perelman, D., Kanaoka, Y., Sangiovanni, J.P., Gronert, K., Smith, L.E., 2011. 5-Lipoxygenase metabolite 4-HDHA is a mediator of the antiangiogenic effect of omega-3 polyunsaturated fatty acids. Sci. Transl. Med. 3, 69ra12.

Sapieha, P., Chen, J., Stahl, A., Seaward, M.R., Favazza, T.L., Juan, A.M., Hatton, C.J., Joyal, J.S., Krah, N.M., Dennison, R.J., Tang, J., Kern, T.S., Akula, J.D., Smith, L.E., 2012. Omega-3 polyunsaturated fatty acids preserve retinal function in type 2 diabetic mice. Nutr. Diabetes 2, e36.

Sato, T., Wada, K., Arahori, H., Kuno, N., Imoto, K., Iwahashi-Shima, C., Kusaka, S., 2012. Serum concentrations of bevacizumab (avastin) and vascular endothelial growth factor in infants with retinopathy of prematurity. Am J. Ophthalmol. 153 (327–333), e1.

Schoonjans, K., Peinado-Onsurbe, J., Lefebvre, A.M., Heyman, R.A., Briggs, M., Deeb, S., Staels, B., Auwerx, J., 1996. PPARalpha and PPARgamma activators direct a distinct tissue-specific transcriptional response via a PPRE in the lipoprotein lipase gene. EMBO J. 15, 5336–5348.

Shao, Z., Friedlander, M., Hurst, C.G., Cui, Z., Pei, D.T., Evans, L.P., Juan, A.M., Tahiri, H., Duhamel, F., Chen, J., Sapieha, P., Chemtob, S., Joyal, J.S., Smith, L.E., 2013. Choroid sprouting assay: an ex vivo model of microvascular angiogenesis. PLoS One 8, e69552.

Shao, Z., Fu, Z., Stahl, A., Joyal, J.S., Hatton, C., Juan, A., Hurst, C., Evans, L., Cui, Z., Pei, D., Gong, Y., Xu, D., Tian, K., Bogardus, H., Edin, M.L., Lih, F., Sapieha, P., Chen, J., Panigrahy, D., Hellstrom, A., Zeldin, D.C., Smith, L.E., 2014. Cytochrome P450 2C8

omega3-long-chain polyunsaturated fatty acid metabolites increase mouse retinal pathologic neovascularization–brief report. Arterioscler. Thromb. Vasc. Biol. 34, 581–586.
Simo, R., Simo-Servat, O., Hernandez, C., 2015. Is fenofibrate a reasonable treatment for diabetic microvascular disease? Curr. Diab. Rep. 15, 24.
Smith, L.E., Wesolowski, E., Mclellan, A., Kostyk, S.K., D'amato, R., Sullivan, R., D'amore, P.A., 1994. Oxygen-induced retinopathy in the mouse. Invest. Ophthalmol. Vis. Sci. 35, 101–111.
Stahl, A., Connor, K.M., Sapieha, P., Willett, K.L., Krah, N.M., Dennison, R.J., Chen, J., Guerin, K.I., Smith, L.E., 2009. Computer-aided quantification of retinal neovascularization. Angiogenesis 12, 297–301.
Stahl, A., Connor, K.M., Sapieha, P., Chen, J., Dennison, R.J., Krah, N.M., Seaward, M.R., Willett, K.L., Aderman, C.M., Guerin, K.I., Hua, J., Lofqvist, C., Hellstrom, A., Smith, L.E., 2010. The mouse retina as an angiogenesis model. Invest. Ophthalmol. Vis. Sci. 51, 2813–2826.
Stahl, A., Krohne, T.U., Sapieha, P., Chen, J., Hellstrom, A., Chew, E., Holz, F.G., Smith, L.E., 2011. Lipid metabolites in the pathogenesis and treatment of neovascular eye disease. Br. J. Ophthalmol. 95, 1496–1501.
Suzuki, M., Ozawa, Y., Kubota, S., Hirasawa, M., Miyake, S., Noda, K., Tsubota, K., Kadonosono, K., Ishida, S., 2011. Neuroprotective response after photodynamic therapy: role of vascular endothelial growth factor. J. Neuroinflammation 8, 176.
Szymczak, M., Murray, M., Petrovic, N., 2008. Modulation of angiogenesis by omega-3 polyunsaturated fatty acids is mediated by cyclooxygenases. Blood 111, 3514–3521.
Tsao, C.C., Coulter, S.J., Chien, A., Luo, G., Clayton, N.P., Maronpot, R., Goldstein, J.A., Zeldin, D.C., 2001. Identification and localization of five CYP2Cs in murine extrahepatic tissues and their metabolism of arachidonic acid to regio- and stereoselective products. J. Pharmacol. Exp. Ther. 299, 39–47.
Varet, J., Vincent, L., Mirshahi, P., Pille, J.V., Legrand, E., Opolon, P., Mishal, Z., SORIA, J., Li, H., Soria, C., 2003. Fenofibrate inhibits angiogenesis in vitro and in vivo. Cell. Mol. Life Sci. 60, 810–819.
Walsky, R.L., Gaman, E.A., Obach, R.S., 2005. Examination of 209 drugs for inhibition of cytochrome P450 2C8. J. Clin. Pharmacol. 45, 68–78.
Wang, Z., Moran, E., Ding, L., Cheng, R., Xu, X., Ma, J.X., 2014. PPARalpha regulates mobilization and homing of endothelial progenitor cells through the HIF-1alpha/SDF-1 pathway. Invest. Ophthalmol. Vis. Sci. 55, 3820–3832.
Wong, T.Y., Simo, R., Mitchell, P., 2012. Fenofibrate - a potential systemic treatment for diabetic retinopathy? Am J. Ophthalmol. 154, 6–12.
Yanai, R., Mulki, L., Hasegawa, E., Takeuchi, K., Sweigard, H., Suzuki, J., Gaissert, P., Vavvas, D.G., Sonoda, K.H., Rothe, M., Schunck, W.H., Miller, J.W., Connor, K.M., 2014. Cytochrome P450-generated metabolites derived from omega-3 fatty acids attenuate neovascularization. Proc. Natl. Acad. Sci. U. S. A. 111, 9603–9608.
Yang, X., Gong, Y., Friesel, R., 2011. Spry1 is expressed in hemangioblasts and negatively regulates primitive hematopoiesis and endothelial cell function. PLoS One 6, e18374.
Yang, X., Gong, Y., Tang, Y., Li, H., He, Q., Gower, L., Liaw, L., Friesel, R.E., 2013. Spry1 and Spry4 differentially regulate human aortic smooth muscle cell phenotype via Akt/FoxO/myocardin signaling. PLoS One 8, e58746.
Yu, J.Y., Lyons, T.J., 2013. Modified lipoproteins in diabetic retinopathy: a local action in the retina. J. Clin. Exp. Ophthalmol 4.
Zhang, G., Panigrahy, D., Mahakian, L.M., Yang, J., Liu, J.Y., Stephen Lee, K.S., Wettersten, H.I., Ulu, A., Hu, X., Tam, S., Hwang, S.H., Ingham, E.S., Kieran, M.W., Weiss, R.H., Ferrara, K.W., Hammock, B.D., 2013. Epoxy metabolites of docosahexaenoic acid (DHA) inhibit angiogenesis, tumor growth, and metastasis. Proc. Natl. Acad. Sci. U. S. A. 110, 6530–6535.